Crystalline silicon surface passivation by thermal ALD deposited Al doped ZnO thin films

Jagannath Panigrahi, Vandana, Rajbir Singh, C. M. S. Rauthan, and P. K. Singh

Citation: AIP Advances **7**, 035219 (2017);
View online: https://doi.org/10.1063/1.4979326
View Table of Contents: http://aip.scitation.org/toc/adv/7/3
Published by the American Institute of Physics

Crystalline silicon surface passivation by thermal ALD deposited Al doped ZnO thin films

Jagannath Panigrahi,[1,2] Vandana,[1,2,a] Rajbir Singh,[1,2] C. M. S. Rauthan,[1,2] and P. K. Singh[1,2,a,b]

[1]*Academy of Scientific and Innovative Research (AcSIR), CSIR-National Physical Laboratory Campus, New Delhi 110012, India*

[2]*Inorganic Photovoltaic Devices Group, Advanced Materials and Devices Division, CSIR-National Physical Laboratory, Network of Institute for Solar Energy, New Delhi 110012, India*

(Received 16 November 2016; accepted 17 February 2017; published online 27 March 2017)

The evidence of good quality silicon surface passivation using thermal ALD deposited Al doped zinc oxide (AZO) thin films is demonstrated. AZO films are prepared by introducing aluminium precursor in between zinc and oxygen precursors during the deposition. The formation of AZO is confirmed by ellipsometry, XRD and Hall measurements. Effective minority carrier lifetime (τ_{eff}) greater than 1.5ms at intermediate bulk injection levels is realized for symmetrically passivated p-type silicon surfaces under optimised annealing conditions of temperature and time in hydrogen ambient. The best results are realised at 450°C annealing for >15min. Such a layer may lead to implied open circuit voltage gain of 80mV. [http://dx.doi.org/10.1063/1.4979326]

The unsatisfied dangling bonds at the crystalline silicon surface introduce very high density of energy levels (~ $10^{15}cm^{-2}eV^{-1}$) inside the forbidden bandgap which are referred to as surface or interface states (D_{it}). These states greatly enhance electron-hole recombination at the surface. This defect mediated recombination at the surface can be described using Shockley-Read-Hall (SRH) statistics.[1] The reduction of surface recombination is referred to as surface passivation. The passivation quality of the surface is determined by the parameter effective surface recombination velocity (S_{eff}). Since each recombination event at the surface requires one electron and one hole in addition to an interface state, two fundamental approaches to passivation are; i) chemical passivation to reduce the density of interface states or, ii) field effect passivation to reduce concentration of one or the other carrier at the surface.[2] The first strategy is achieved by growth of a thin dielectric or semiconducting layer on the silicon surface. Remaining dangling bonds are passivated by the hydrogen atoms from within the passivating layer itself or externally via annealing in a hydrogen environment. By this means, interface states density is reduced to extremely low levels (~$10^{10}cm^{-2}$). The second approach is accomplished by built-in charges within a passivating layer or stack on the surface. The S_{eff} decreases with the inverse square of the charge density whereas it decreases with inverse of the interface states density as can be deduced from the SRH statistics. Improvements in the passivation of crystalline silicon surface is one of the thrust area for efficiency gain and cost reduction in industrial crystalline silicon (c-Si) solar cells.[3] Surface recombination on the rear of a c-Si solar cell has a high impact on the efficiency of a c-Si solar cell, especially when the thickness is reduced further.[4] The recent industry standard aluminium back surface field (Al-BSF) has S_{eff} of ~300-600cm/s and by lowering this value to 10-100cm/s, a significant gain in the solar cell conversion efficiency can be achieved. Thin nano layer(s) of dielectric such as AlO_x, SiO_x and SiN_x are the key component in

[a]E-mail: vandana1@nplindia.org, pksnpl16@gmail.com

[b]Formerly associated with NPL and AcSIR.

today's industrial high efficiency silicon solar cells (such as passivated emitter and rear cell or PERC) due to their excellent material properties desirable for both field effect and chemical passivation. However, a charged passivation layer is unable to passivate p- and n-type simultaneously because of the sub-surface recombination in the inversion layer (e.g., high density of positive charge on p-Si surface).[5] Therefore, excellent chemical passivation achieving very low density of interface states is required in passivation layers containing negligible charge. The possibility to modify the fixed charge density or achieving zero-charge surface passivation has been shown by introducing nano-layers of SiO_x or HfO_x underneath the negatively charged AlO_x layers.[6,7] However, a single layer is always desired to achieve the required surface passivation to avoid process complexity. Nano-layers of semiconducting a-Si:H has been shown to achieve high level of surface passivation by suppressing the interface states, for example in the heterojunction (HIT) solar cells[8] Furthermore, novel high efficiency c-Si solar cell concepts such as tunnel oxide passivated contact cells (TOPCon) or selective contact cells utilise the excellent passivation of the two wafer surfaces combined with a reduction in carrier recombination underneath the contacts.[9] This concept requires layer of a material which is both electrically conductive and would also provide very high level of surface passivation. Al doped zinc oxide (AZO) being a transparent conducting oxide (TCO), has wide range of application in photovoltaics such as: CIGS, a-Si, organic and c-Si based heterojunction solar cells.[10] The band offset of AZO to Si suggests that it could be utilized as a carrier-selective contact.[9] Few studies of AZO as a carrier selective layer with additional passivation layer such as a-Si[11] or Al_2O_3[12] adjacent to Si are available. In the recent past, sol-gel derived AZO films have been explored for the application in c-Si solar cell both as a passivation and antireflection layer.[13] However, there is no report on AZO by atomic layer deposition (ALD) for surface passivation to c-Si which is much superior in terms of quality as compared to the sol-gel based AZO.

The unique features of ALD such as time sequenced cyclic injection of precursors and surface reaction limited growth enable deposition of ultrathin layers, multilayers/nano-laminates and stacks of materials even on highly complex large area surfaces which have found promising application in photovoltaics.[14] The c-Si surface is, generally, modified (pyramidal, nano-texture, nanowires etc.) to reduce the reflection losses from the surface. ALD process can be used to deposit highly uniform and conformal coating on such large area surfaces. For example, the cyclic deposition process enables doping of Al in ZnO by simply injecting the Al precursor after a fixed number of ALD cycles of ZnO, thus AZO films with wide range of Al composition can be made.[15] This study demonstrates the evidence of ALD deposited AZO thin films for the application in c-Si surface passivation and the mechanism is emphasized.

The AZO films are deposited by thermal ALD technique in the form of ZnO/AlO_x multilayers on p-Si (300μm thick, <100> FZ Si, 50 mm diameter, 5Ω-cm) wafers. The wafers are cleaned in a piranha solution followed by dip in buffered HF for 2s, rinse with deionized water. Diethyl Zinc (DEZ) and Trimethyl Aluminium (TMA) are the precursors for Zn and Al respectively and the oxidant is water. Substrate temperature is kept at 150°C during the deposition. Doping of Al in ZnO thin films is conducted via alternate deposition of 15 numbers of DEZ with oxidant cycles followed by 1 ALD cycle of TMA and H_2O. This being one super-cycle, the process is carried out to 16 times (Fig. 1). Identical AZO films are deposited on both sides of the wafer to create symmetrically passivated Si surfaces. Films are characterised by variable angle spectroscopic ellipsometry (VASE, M-2000U, M/s J.A.Woollam Co Inc., USA) in a rotating compensator configuration, grazing incidence X-ray

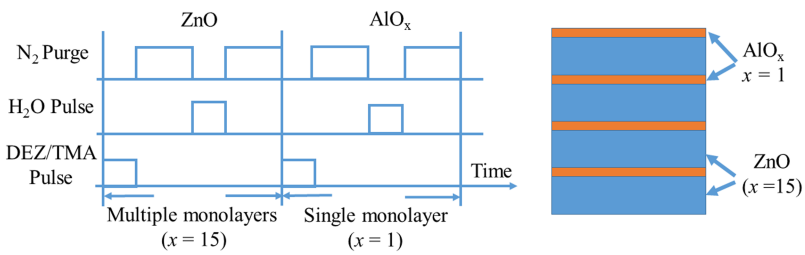

FIG. 1. Schematic of the composition of the ALD cycles for the deposition of AZO thin films.

TABLE I. Comparison of the optical, electrical and structural parameters of as-deposited ZnO and AZO films.

Sample	Al (atomic %)	GPC (Å/cycle)	n (@630nm)	E_g (eV)	N_{Hall} (cm^{-3})	μ_{Hall} (cm^2/V-s)	d_{100} (Å)	D_{100} (nm)
ZnO (300 cycle)	0	2.0	2.0	3.27	3×10^{18}	9	3.241	20
AZO ((15+1)×16)	3.2	1.44	1.88	3.45	8.2×10^{19}	2.5	3.222	15

diffraction technique (GIXRD, Panalytical Xpert Pro) and Hall effect measurement. Post deposition annealing (PDA) is carried out in H_2 ambient (>99.999% purity, from a hydrogen generator) in a tube furnace in the temperature range of 350-500°C (steps of 50°C) where annealing time is varied from 15 to 105 min. The effective minority carrier lifetime (τ_{eff}) is measured using a Sinton's lifetime tester (WCT-120) in transient and quasi-steady-state (QSS) mode depending on the lifetime value.

The measured values of various parameters-growth per cycle (GPC), refractive index, band gap etc. of ZnO (without Al layer) and AZO films deposited on Si substrate are listed in Table I. The thickness of the AZO film is found to be 36.8 (±0.2) nm. The nominal composition of Al in the AZO thin films is determined from the number of DEZ and TMA cycle and is found 3.2% using the relation;[15]

$$Al\ at.\ \% = \frac{GPC_{AlOx}}{GPC_{AlOx} + x \times GPC_{ZnO}}$$

Hall measurement data shows higher carrier concentration for the AZO film (~ $8\times10^{19}cm^{-3}$) as compared to the pure ZnO film (~ $3\times10^{18}cm^{-3}$) which confirms the substitution of the dopant whereas the lower mobility (2.5 cm^2/V-s) compared to ZnO (9 cm^2/V-s) is attributed to the dominant scattering at the interface of ZnO and AlO_x layers and smaller grain size.

The as-deposited films are oriented in (100) plane, the intensity of which is lowered after Al doping whereas reflection from (002) is absent in the doped film (Fig. 2a). A shift in the characteristic 2θ positions of (100) and (101) reflections is observed in the AZO film which is reflected in d_{100}-spacing (=3.22 Å and 3.24 Å for AZO and i-ZnO respectively). This shrinkage in d-spacing (~ 0.02 Å) confirms Al doping in the film where Zn^{2+} ions are substituted by Al^{3+} ions in the ZnO lattice because of their smaller ionic radii. This results as a shift in diffraction angles to the higher values and the substitutional Al acts as an electron donor, contributing to the higher electron concentration. The larger crystallite size (20nm) for ZnO compared to AZO (15nm) suggest the presence of more number of grain boundaries in the doped film which results in lower mobility. Current density-voltage measurement on the test structure In/AZO/p-Si/GaIn structure shows sufficient high current density of ~20mA/cm^2 at 0.7V. The non-ideal Ohmic contacts to the AZO and Si in this case might play some role in lowering the current density.

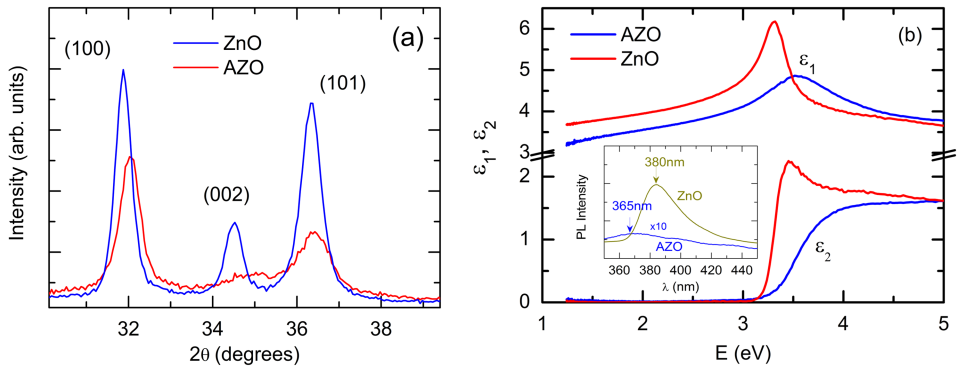

FIG. 2. (a) GI-XRD spectra of ZnO and AZO film on Si. A positive shift in the 2θ position of (100) diffraction peak is observed in AZO. (b) Dielectric functions (ε_1 and ε_2) determined by modelling the spectroscopic ellipsometry data using a combination of oscillators.[16] Inset shows the PL spectra indicating absence of exciton emission in AZO.

Fig. 2b shows the real (ε_1) and imaginary (ε_2) parts of the dielectric functions of the films extracted from ellipsometry data using a combination of oscillators.[16,17] The blue shift in the peak position in ε_1 implies increase in band gap with doping. In general, the broadening parameter of a transition peak is inversely proportional to the lifetime of carriers or excitons. This implies that the lifetime of excitons becomes shorter as the electron concentration increases. The absence of excitonic peak signatures in the ε_2 spectra of AZO films also confirms this fact. This nature is also confirmed from the PL spectrum (inset of Fig. 2b) wherein no blue emission, which is a characteristic of i-ZnO films, is observed in AZO.

The passivation quality of a surface is quantified by S_{eff}. Other parameters are also the recombination current density (J_0) and implied open-circuit voltage (iV_{oc}). However, the directly measured parameter is the effective minority carrier lifetime (τ_{eff}) which comprises several recombination terms:

$$\frac{1}{\tau_{eff}} = \frac{1}{\tau_{radiative}} + \frac{1}{\tau_{Auger}} + \frac{1}{\tau_{SRH}} + \frac{2S_{eff}}{W}$$

Where the first two terms on the right comprise the intrinsic recombination in Si and can be calculated using empirical parameterisation of Kerr[18] or Richter,[19] the third term is represents SRH recombination in bulk and the last term represents the surface recombination. Injection level (Δn) dependent τ_{eff} of the symmetrically passivated sample is measured in quasi-steady state (QSS) and transient (tr) mode. For simplicity only the τ_{eff} value at a particular Δn is taken. The uncertainty in the measured τ_{eff} values is ±11% when measured in QSS mode and ±8% for the transient mode.[20] The average τ_{eff} values at $\Delta n = 5\times10^{14}cm^{-3}$ in as-deposited AZO passivated sample is 8-10μs which improves after annealing as can be seen from Fig. 3a. This improvement in passivation after annealing in hydrogen environment must be due to the inter-diffusion of H-atoms towards the Si surface and bonding with the un-coordinated Si atoms. Hence the mechanism here could be the chemical passivation. The annealing temperature (T_{anl}) and time (t_{anl}) determine the degree of surface passivation, implying a thermally activated reaction associated with chemical passivation. At all T_{anl}, the τ_{eff} value shows a rising trend initially with t_{anl} (up to 15 min), and further increase in t_{anl} (up to 45 min) the τ_{eff} is almost the same within measurement uncertainties. τ_{eff} values do not improve much (~ 70μs) with t_{anl} till $T_{anl} < 350°C$. Annealing temperatures around 450°C gives the best passivation results. The highest τ_{eff} at each T_{anl} is achieved for t_{anl} between 30-45min. The effective lifetime of sample annealed at 450°C for different duration shows an increasing trend from τ_{eff} = 10μs in as-deposited sample to a maximum τ_{eff} value ≈ 1.6ms (S_{eff} ~ 10cm/s) after 45 min of annealing. This is probably the highest values for silicon surface passivation demonstrated using ALD deposited AZO thin films. With further rise in t_{anl}, τ_{eff} decreases to 860μs (after 90 min) but still this value is much higher compared to the value of as-deposited samples.

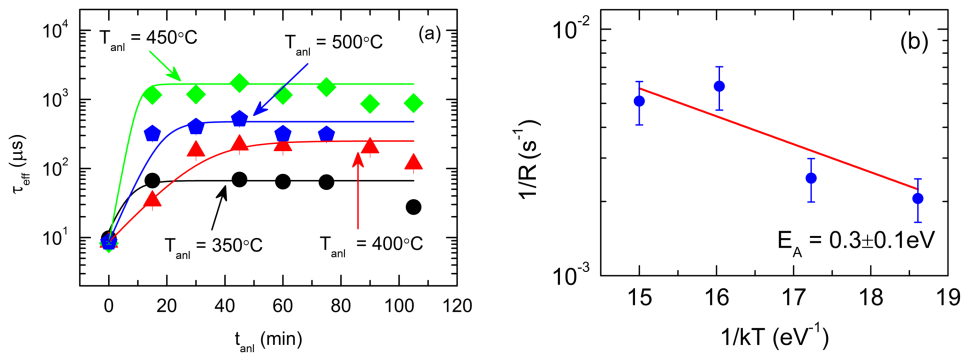

FIG. 3. (a) Effective minority carrier lifetime (τ_{eff}) of symmetrically passivated p-Si at the bulk injection level $\Delta n = 5\times10^{14}cm^{-3}$. The uncertainties in the τ_{eff} values is ±8%. The samples are annealed at different temperatures (T_{anl}) for various time durations (t_{anl}). The lines using eq. (1) give the best fit to the measured data points. (b) Arrhenius plot of the reaction rate (solid circles) for determination of activation energy of hydrogen diffusion for a 30nm AZO film on p-Si. Reaction rate is determined from fitting of data shown in Fig. 3a using equation (1).

The passivation reaction can be modelled using the expression proposed by Mitchell et al.,[21] where τ_{eff} is a function of both t_{anl} and T_{anl}:

$$\frac{1}{\tau_{eff}} = \left[a + b\exp\left(-\frac{t_{anl}}{R}\right)\right]. \quad (1)$$

$$\frac{1}{R} = Cexp(-E_A/kT_{anl}). \quad (2)$$

where, R represents the reaction time constant for passivation or the rate of hydrogen inter-diffusion towards the silicon interface. The parameters "a" and "b" are some constants. E_A is the activation energy of the reactions dependent on temperature. The eq. (1) is fitted to τ_{eff} values at each T_{anl} and the rate of reaction R is determined (Fig. 3a). The extracted R is plotted as a function of inverse temperature in Fig. 3b. Using eq. (2), the activation energy E_A is determined. The activation energy is found to be 0.3±0.1eV. In the case of a-Si:H passivation E_A = 0.7eV is found by Mitchell et al.,[21] whereas for Ga_2O_3, Allen et al., has reported E_A = 0.5eV.[22] For Al_2O_3 passivation E_A is found equal to 1.3eV.[23] On the other hand, for Al_2O_3/SiO_2 stack, the corresponding value is 0.9eV.[24] The applied fit function eq.(1) is different in these different investigations.

The hydrogenation of interface defects is a temperature activated process with a characteristic activation energy, which involves the transport of hydrogen atoms towards the interface and their interaction with dangling bonds at the Si surface. Annealing supports the hydrogenation of the interface, however, at the same time it leads to out-diffusion and hydrogen loss. At higher temperature Si-H bond is unstable resulting in the out-diffusion and consequently degradation in the level of passivation. In addition to annealing temperature, hydrogenation of the interface is also dependent on the material properties such as microstructure, density and thickness. For example, denser and thicker films prevent hydrogen out-diffusion during high temperature annealing process whereas in the case of low density films, hydrogenation occurs readily often at lower temperatures. The higher activation energies of passivation reaction are reported in CVD deposited a-Si:H, ALD Al_2O_3 and Ga_2O_3, PECVD SiN_x films[21–24] which are generally amorphous. On the other hand, ALD deposited AZO films are polycrystalline in nature as confirmed by the X-ray diffraction data and with annealing the crystallinity improves. Therefore, the transportation of H species through grain boundary diffusion prevails which could be the reason for the lower value of activation energy. Another assumption supporting the passivation of surface states by AZO may also be the presence of Al which acts as catalyst for the production of atomic hydrogen. The same mechanism has been proposed in the case of "alneal" scheme where the forming gas annealing of thermal SiO_2 with the presence of a thin evaporated Al layer reduced the surface states density to $\sim 10^9 cm^{-2}eV^{-1}$.[25] The lifetime values of Si symmetrically passivated by undoped ZnO annealed in H_2 environment with the same PDA conditions as that of AZO does not give much improved values (max τ_{eff} obtained = 35μs).

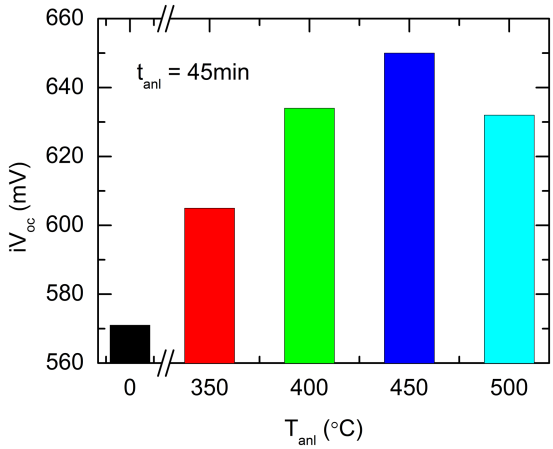

FIG. 4. Implied open circuit voltage (iV_{oc}) of as-deposited (T_{anl} = 0) and annealed (T_{anl} = 350, 450 and 500 °C) samples. The values are given for t_{anl} = 45min.

As the surface is chemically passivated, it can be assumed that there is no surface charge present at the silicon surface such that the concentration of carriers at the surface (n_s) is equal to that at a position slightly below the surface (n_d). Hence, the surface recombination current density (J_{0s}) can be determined for the case where energy band bending at the surface is negligible. Using the approximation according to McIntosh and Black,[26] the calculated J_{0s} is ~13 fA/cm^2 for the sample with highest τ_{eff} after optimum PDA conditions.

For a silicon solar cell the term implied open circuit voltage (iV_{oc}) represents the same behaviour as τ_{eff} or S_{eff} represent for a symmetrically passivated Si.[27] The iV_{oc} can be estimated from the measured injection level dependent minority carrier lifetime. The corresponding implied open circuit voltage (iV_{oc}) would increase from ~ 570mV to ~ 650mV if a quality passivation (S_{eff} < 10cm/s) layer is applied on a solar cell as can be seen from Fig. 4. The level of surface passivation of our samples did not deteriorate with time and is found to remain constant.

In summary, Al rich ZnO (AZO) films are made using ALD. The XRD data shows that the d-spacing is small in comparison with pure ZnO films. In addition, increase in carrier concentration and band gap is observed with the increase in Al concentration. The effective minority carrier lifetime greater than 1.5ms in p-type silicon is realized after annealing of the AZO films in hydrogen ambient for > 20 min at 450°C. The activation energy of the passivation reaction is found to be 0.3eV which is low due to the presence of Al which act as catalyst for the production of atomic hydrogen or due to the presence of grain boundaries. This present study suggests that these films are suitable for the application of AZO for surface passivation in wafer based crystalline silicon solar cells.

This work is carried out for the project NWP55 funded by Council of Scientific and Industrial Research (CSIR) under its solar initiative "Technologies and Products for Solar Energy Utilization through Networks" [***TAP-SUN***]. The financial support from this project to JP and RS is also acknowledged.

[1] A. G. Aberle, S. Glunz, and W. Warta, Sol. Energy Mater. Sol. Cells **29**, 175 (1993).
[2] A. G. Aberle, Prog. Photovoltaics Res. Appl. **8**, 473 (2000).
[3] T. Dullweber and J. Schmidt, IEEE J. Photovoltaics **6**, 1366 (2016).
[4] M. A. Green, Prog. Photovoltaics Res. Appl. **7**, 327 (1999).
[5] S. Dauwe, L. Mittelstädt, A. Metz, and R. Hezel, Prog. Photovoltaics Res. Appl. **10**, 271 (2002).
[6] G. Dingemans, N. M. Terlinden, M. A. Verheijen, M. C. M. Van De Sanden, and W. M. M. Kessels, J. Appl. Phys. **110**, 93715 (2011).
[7] D. K. Simon, P. M. Jordan, I. Dirnstorfer, F. Benner, C. Richter, and T. Mikolajick, Sol. Energy Mater. Sol. Cells **131**, 72 (2014).
[8] M. Taguchi, A. Yano, S. Tohoda, K. Matsuyama, Y. Nakamura, T. Nishiwaki, K. Fujita, and E. Maruyama, IEEE J. Photovoltaics **4**, 96 (2014).
[9] P. Stradins, S. Essig, W. Nemeth, B. G. Lee, D. Young, A. Norman, Y. Liu, J.-W. Luo, E. Warren, A. Dameron, V. LaSalvia, M. Page, A. Rohatgi, A. Upadhyaya, B. Rounsaville, Y.-W. Ok, S. W. Glunz, J. Benick, F. Feldmann, and M. Hermle, 6th WCPEC, Japan, Kyoto, 2014.
[10] E. Fortunato, D. Ginley, H. Hosono, and D. C. Paine, MRS Bulletin **32**, 242 (2007).
[11] F. Feldmann, K. U. Ritzau, M. Bivour, A. Moldovan, S. Modi, J. Temmler, M. Hermle, and S. W. Glunz, Energy Procedia **77**, 263 (2015).
[12] D. Garcia-Alonso, S. Smit, S. Bordihn, and W. M. M. Kessels, Semicond. Sci. Technol. **28**, 82002 (2013).
[13] F. Khan, Vandana, S. N. Singh, M. Husain, and P. K. Singh, Sol. Energy Mater. Sol. Cells **100**, 57 (2012).
[14] J. A. van Delft, D. Garcia-Alonso, and W. M. M. Kessels, Semicond. Sci. Technol. **27**, 74002 (2012).
[15] P. Banerjee, W.-J. Lee, K. Bae, S. B. Lee, and G. W. Rubloff, J. Appl. Phys. **108**, 43504 (2010).
[16] H. C. M. Knoops, B. W. H. van de Loo, S. Smit, M. V. Ponomarev, J.-W. Weber, K. Sharma, W. M. M. Kessels, and M. Creatore, J. Vac. Sci. Technol. A Vacuum, Surfaces, Film **33**, 21509 (2015).
[17] H. Fujiwara and M. Kondo, Phys. Rev. B - Condens. Matter Mater. Phys. **71**, 1 (2005).
[18] M. J. Kerr and A. Cuevas, J. Appl. Phys. **91**, 2473 (2002).
[19] A. Richter, S. W. Glunz, F. Werner, J. Schmidt, and A. Cuevas, Phys. Rev. B - Condens. Matter Mater. Phys. **86**, 1 (2012).
[20] A. L. Blum, J. S. Swirhun, R. A. Sinton, F. Yan, S. Herasimenka, T. Roth, K. Lauer, J. Haunschild, B. Lim, K. Bothe, Z. Hameiri, B. Seipel, R. Xiong, M. Dhamrin, and J. D. Murphy, IEEE J. Photovoltaics **4**, 525 (2014).
[21] J. Mitchell, D. Macdonald, and A. Cuevas, Appl. Phys. Lett. **94**, 162102 (2009).
[22] T. G. Allen and A. Cuevas, Appl. Phys. Lett. **105**, 031601 (2014).
[23] A. Richter, J. Benick, M. Hermle, and S. W. Glunz, Appl. Phys. Lett. **104** (2014).
[24] G. Dingemans, F. Einsele, W. Beyer, M. C. M. Van de Sanden, and W. M. M. Kessels, J. Appl. Phys. **111**, 93713 (2012).
[25] W. D. Eades and R. M. Swanson, J. Appl. Phys. **58**, 4267 (1985).
[26] K. R. McIntosh and L. E. Black, J. Appl. Phys. **116**, 014503 (2014).
[27] R. Sinton and A. Cuevas, 16th European PVSEC, Glasgow, UK (2000).